

# EVALUATION OF SELECTED METHODS FOR EXTRACTING DIGITAL TERRAIN MODELS FROM SATELLITE BORN DIGITAL SURFACE MODELS IN URBAN AREAS

Thomas Krauß, Hossein Arefi, Peter Reinartz

German Aerospace Center (DLR), Remote Sensing Technology Institute, D-82234 Weßling, Germany  
E-Mail: Thomas.Krauss@dlr.de

## Commission I/4

**KEY WORDS:** digital surface models, digital terrain models, urban areas, simulation

### ABSTRACT:

For the generation of 3D city models from satellite stereo imagery beyond the generation of digital surface models (DSM) from stereo data the next crucial step is the separation of urban 3D objects from ground. To do this the most common method is the derivation of a so called digital terrain model (DTM) from the DSM. The DTM should ideally contain only the surface of the ground on which the urban objects are located. Since only the surface of the objects can be seen from space, sophisticated methods have to be developed to gain information of the bare ground. In this paper selected methods for the extraction of a DTM from a DSM are described and evaluated. The evaluation is done by applying the methods to synthetically generated DSMs. These synthetical DSMs are a combination of ground and typical urban objects put on top of it. The application of the DTM extraction methods should recover in turn the original ground model as good as possible. Also the sum of the obtained DTM and the profile of the urban objects should reconstruct the original DSM. The profile of the urban objects is often referenced as normalized digital elevation model (nDEM). But in general the equation  $DSM = DTM + nDEM$  is not always valid – especially for buildings situated on the slope of a hill. If the nDEM would simply be the difference of  $DSM - DTM$  the slope of the hill – contained in the DTM – will be reflected on the roof of the buildings. So also an advanced method for derivation of the nDEM from DSM and DTM is presented and tested.

## 1 INTRODUCTION

Since the 1980s there is intense research on digital terrain models (DTMs) (Li et al., 2005). Since then DTMs are generated from direct terrain measurements or extracted from digital surface models (DSMs). DSMs origin mostly from laser scanning, radar interferometry or from stereo processing of optical aerial or satellite imagery. DSMs represent the surface of all objects on the ground while a DTM should only represent the ground information without any objects located on it.

A DTM can be derived from a DSM by detecting and removing all objects and filling these areas in an intelligent manner. The problem of generating a DTM from an existing DSM is therefore mainly the detection of off-ground objects. Beside the classical method of removing elevated objects manually also a wide variety of DSM filtering algorithms where developed.

These methods exploit some characteristic features of the objects which have to be removed. Most of these methods were developed in the last decade for filtering laser scanning data which are currently one of the most precise sources of DSM data. In our paper we simulate DSMs emulating such ones as generated from very high resolution optical stereo satellite imagery with ground sampling distances (GSD) of about 0.5 to 1 m. Such DSMs are generated by dense stereo methods which generate normally high quality DSMs with GSDs of about 2 to 5 times of the GSD of the original imagery. But these methods tend to introduce many holes, blunders and occlusions especially in urban areas (dAngelo et al., 2008).

In this paper we compare three selected DTM extraction methods using synthetically generated DSMs. On top of generated DTMs we add urban-type objects (DEM) to generate the synthetical DSMs. Since the original synthetic DTM (ground) and also the DEMs of the objects are known we are able to evaluate the capabilities and limitation of the investigated methods by comparing

the DTMs extracted by the algorithms with our synthetically generated ones. Beside this we are also able to add noise, holes or occlusions to the synthetical DSMs and evaluate the sensitivity of the methods to such typical DSM generation errors.

The investigated methods where selected for usability in an automatic processing chain for urban city modeling from very high resolution stereo satellite imagery. Therefore we choose:

- The Classical morphological approach (Weidner and Förstner, 1995)
- Geodesic dilation (Arefi et al., 2007)
- Steep edge detection (Krauß and Reinartz, 2010)

### 1.1 Basic considerations

First we need to introduce a new method for extracting the normalized digital elevation model (nDEM) from DSM and DTM. The nDEM represents the elevated objects removed from the DSM to gain the DTM. Normally the nDEM is simply derived as

$$nDEM = DSM - DTM$$

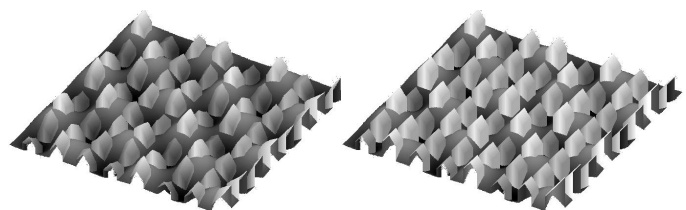


Figure 1: Synthetically generated DSM composed from hip roof houses (nDEM) and a rolling ground (DTM) – left: simple DTM+nDEM, right: correctly added nDEM to max(DTM) in each building area

which does not work for non-flat DTMs. If we use the inverse  $DSM = DTM + nDEM$  to generate the synthetical DSMs we will gain houses with roofs reflecting the ground variations (fig. 1, left).

Therefore we propose to use an object based ground detection to detect the lowest point in the footprint of a nDEM object  $i$  and remove this minimum value as constant DTM from the whole object  $i$ :

$$nDEM_i = DSM - \min_i DTM_i$$

The objects  $i$  (fig. 2, left) are now put on these locally flattened  $DTM_i$  parts (fig. 2, center) to generate the correct DSM (figs. 1, 2, right).

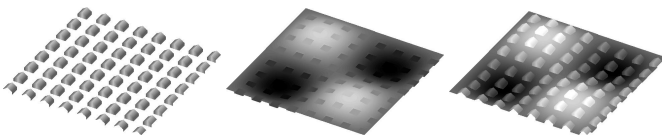


Figure 2: Correct nDEM fusion/extraction: detect objects (left), search for lowest height of each object in DTM and put footprint of object to this level (center), add/subtract objects onto these “baseplate” levels (right)

## 1.2 Preliminary work

Since the separation of ground and elevated objects from DSMs is required for many purposes already since about 30 years algorithms were developed to extract DTMs from DSMs automatically. One of the classic works on this topic can be found in Haralick et al. (1987) later refined in Weidner and Förstner (1995). In the mid 1990s more and more work on this topic flourished especially triggered by the invention and increased use of laser scanning systems (LIDAR). These first – and simplest – approaches were based on a simple morphological opening searching for the lowest values inside a given window. Since this simple method is still one of the best we included it also in our investigations.

A completely other approach was proposed by Axelsson (1999). He builds a type of a convex hull below the DSM by building a irregular network (TIN) and iteratively densifying it limited by a smoothness threshold. An extension to this method is described in Baillard (2008). A slope based filtering method was proposed by Vosselman (2000). He takes the height difference of points within a neighbourhood into account to separate ground and off-ground points. To overcome the problem of the prior determination of the size of the structuring element in the classic approaches Zhang et al. (2003) proposed a progressive morphological filtering method using the classical morphological opening method but gradually increasing the size of the structuring element. The different results are in turn used to separate ground and non-ground points of the DSM.

Later also other approaches depending on height filtering like the morphological reconstruction or geodesic dilation as described in Arefi and Hahn (2005) or Arefi et al. (2009) were developed. On the other hand the algorithm described in Krauß and Reinartz (2010) falls in the category of slope based algorithms since it exploits existing steep walls in urban DSMs. Summarizing these we can distinguish following types of DTM-from-DSM algorithms:

- Algorithms based on horizontal morphology (Haralick et al., 1987), (Zhang et al., 2003)

- Algorithms based on vertical morphology like (Arefi and Hahn, 2005)
- Algorithms based on slopes like (Zhang et al., 2003), (Krauß and Reinartz, 2010)
- Other approaches like Axelsson (1999) or low pass filtering in fourier space ...

In the following investigation we use one representative method of each of the first three types.

## 2 METHODS

### 2.1 Classical morphological approach

The classical morphological approach proposed already by Haralick et al. (1987) and Weidner and Förstner (1995) exploits the fact that buildings need to have a maximum width for daylight illumination from windows to streets and courtyards. So a morphological erosion with a diameter of the structuring element of the estimated largest cross-section of a building is applied to the DSM. In this case all roof points of the buildings get replaced by the lowest (ground) value in distance of half the diameter of the structuring element. Afterwards the erosion is followed by a dilation with the same structuring element to restore the edges of eroded hills. The dilation step was added by Krauß and Reinartz (2009) to reconstruct eroded hills back to their original shape (see fig. 3: green line (only erosion) vs. blue line (added dilation)).

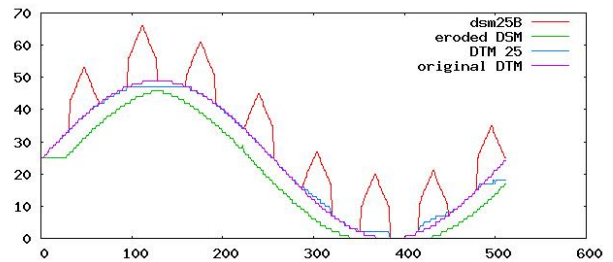


Figure 3: Morphological erosion/dilation of DSMs with radius 35, red: synthetic DSM, green: eroded DSM, blue: derived DTM, purple: original synthetic DTM

Using this morphological opening eliminates all elevated objects smaller than the size of the structuring element. This method works very well in most of all cases. It fails nevertheless if industrial buildings with roof areas larger than the structuring element exist which will not be eliminated or hills smaller than the structuring element will be rubbed out.

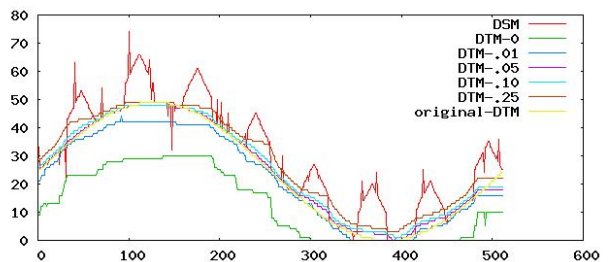


Figure 4: Modified rank median filtering with radius 25 m and ranks 0 %, 1 %, 5 %, 10 % and 25 %; 0 % corresponds to classical erosion/dilation in which case blunders will dominate the derived DTM; at a too high rank (25 %) non-ground objects will dominate

Also noise in the DSM like negative outliers below the ground tend to dominate the DTM if only the classical opening approach

is used. Fig. 4 shows a noisy DSM (red) as common in stereo reconstruction algorithms. Applying a simple “opening” leads to the DTM shown in green – the negative outliers of the noisy DSM dominate the DTM.

To overcome this problem the method has to be changed slightly as proposed in Krauß et al. (2008) by using a low rank median filter of about 1 to 5 % (percentile filter, 50 % corresponds to the median) instead of the erosion and a high rank median of about 95 % instead of the dilation. In this case the outliers contained in the DSM from the DSM generation step will not dominate the created DTM. Fig. 4 shows in blue, purple, cyan and brown the DTMs gained by using 1 %, 5 %, 10 % and 25 % percentiles and the original synthetic DTM in yellow. If the percentile value is chosen too high (like 25 %) the DTM will contain also more and more object artefacts.

## 2.2 Geodesic dilation

The geodesic dilation (Arefi et al., 2007) uses in contrast to the morphological opening not a lateral threshold for the size of the structuring element but a height threshold and follows an iterative application of morphological dilations until stability. The terrain models delivered by this method are mostly very promising. This filtering method is motivated from “Morphological grayscale reconstruction in image analysis: applications and efficient algorithms” of Vincent (1993). The detailed description on this algorithm can be found in Arefi et al. (2009).

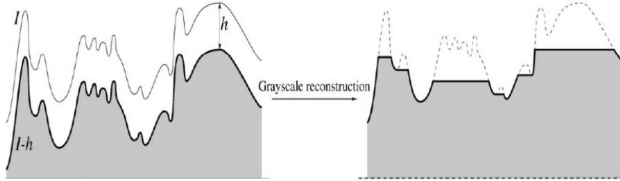


Figure 5: Reconstruction by geodesic dilation of a mask  $I$  from a marker  $J = I - h$  (Arefi et al., 2009)

In short the algorithm can be described as follows: It needs two images, the so called “marker” and “mask” images. The marker image is produced by subtraction of an offset  $h$  from the mask – the input DSM. The value of  $h$  corresponds to the maximum height of the suppressed parts. The marker image is dilated by an elementary isotropic structuring element and the resulting image is forced to remain below the mask image. This means, the mask image acts as a limit for the dilated marker image. Morphology dilation of the marker and point wise minimum between the dilated image and the mask is iterated until stability. The “reconstructed image” corresponds now to the wanted DTM (Arefi et al., 2009). Additionally it is important to mention that the objects connecting to the border of image will not be properly filtered. Therefore, it is important to select an area bigger than the test area to be sure that all the objects are located inside the image.

## 2.3 Steep edge detection

The approach described in Krauß and Reinartz (2010) exploits the fact of existing steep edges in urban DSMs. Subtracting the results of two different sized median or averaging filters show the largest differences beneath steep edges. Thresholding and masking the DSM with these areas results in only ground points near steep edges. Filling this DEM afterwards results in the DTM. Care has to be taken on the sizes of the filters and height-thresholds since also huge objects on top of roofs may be erroneously detected and their foot points (sitting on the roof!) will be taken as ground values. Fig. 7 shows a typical DSM profile of an urban

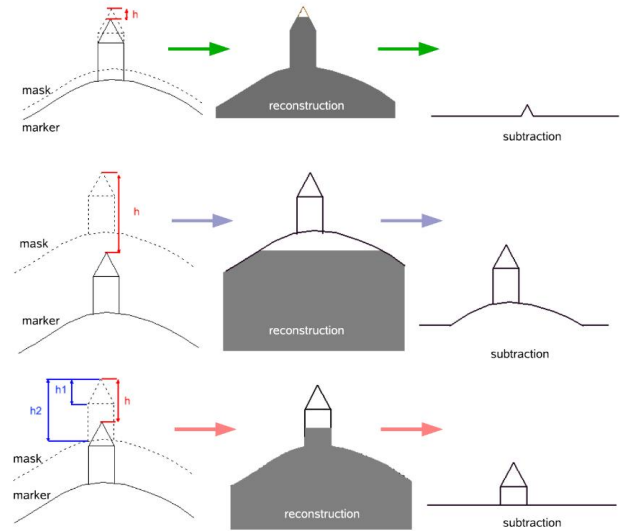


Figure 6: Influence of the selection of the offset parameter  $h$

situation filtered with a median of radius 4 in red. In green the results of applying a median filter of radius 40 is shown and in blue the areas of the DSM satisfying  $M_4 < M_{40} - t$ . These (blue) areas of the DSM are so characterized as “low areas near steep edges” and will be filled and interpolated to the DTM.

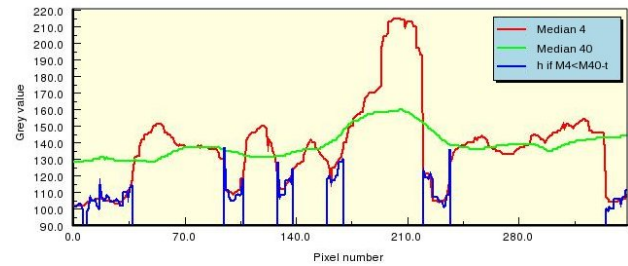


Figure 7: Typical profile showing the calculated medians and the detected street level areas (blue)

Applying two median filters with different sizes show different behaviour at steep edges. The large sized median fills up small holes where the small median filter follows the height structure more strictly. Subtracting the medians and applying a threshold marks areas at the bottom of steep walls. Filling these derived “street level candidates” deliver the DTM. The (small) height threshold of typically 2 to 5 m is needed due to noise artefacts in the DSM. Fig. 8 shows a typical DSM derived from Ikonos satellite stereo images showing the center of Munich with a GSD of about 1 m filtered and interpolated to the resulting DTM.

## 3 SIMULATION MODELS

For the evaluation typical DSMs in a size of  $512 \times 512$  pixels with a simulated resolution of 1 m horizontal and 1 m vertical per digital number are generated. Four types of typical urban DEMs are used:

- Forest area with trees and small paths between ( $64 \text{ m} \times 64 \text{ m}$ , heights 20–30 m)
- Housing area with wide spread houses with gabled roofs ( $16 \text{ m} \times 24 \text{ m}$ , height 10 m plus roof 10 m)
- Industrial area with large flat buildings ( $112 \text{ m} \times 112 \text{ m}$ , height 20 m)
- Urban area with blocks of different height flat roofed buildings ( $5 \times 7$  blocks of  $16 \text{ m} \times 16 \text{ m}$ , heights 20, 25, 30 m)

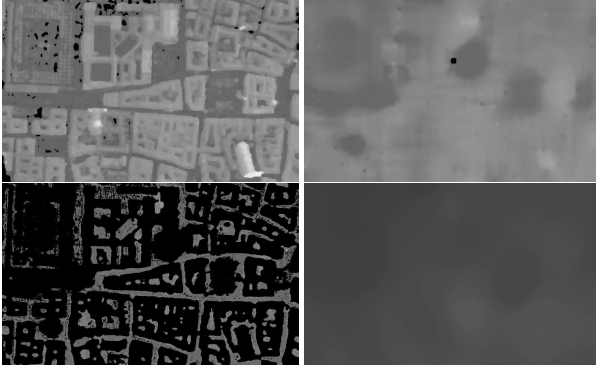


Figure 8: Top: Small (radius 4) median (left), large (radius 40) median (right); Bottom: left: detected “low” areas (typically streets or courtyards) and filled/interpolated DTM (right)

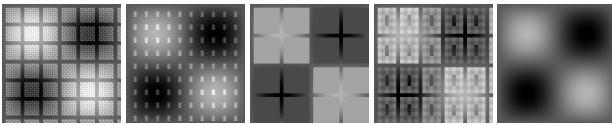


Figure 9: Simulated DSMs with DTM of amplitude 25 m, Forest, Houses, Industry, Urban and synthetic DTM (left to right)

These objects are put on smooth rolling hills with different amplitudes ranging from 0 to 25 m and different frequencies as DTMs. For overlaying of the object DEMs to the DTM the method described in chapter 1.1 using an overlay on objects “base plates” cut out from the DTMs is used in cases Houses, Industry and Urban but not for Forest which follows the DTM.

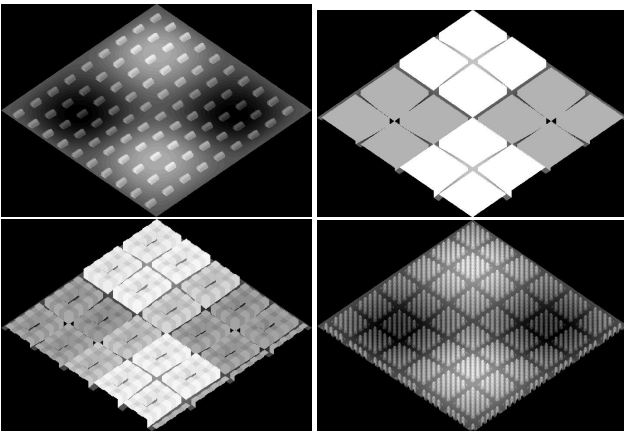


Figure 10: 3D view of simulated typical urban areas: Houses, Industry, Urban, Forest

## 4 RESULTS

### 4.1 Object Type Dependency

In the first evaluation we investigate the behaviour of the different algorithms, referenced throughout this section as

- “opening” for the morphological opening of the classical approach using a radius of 12 m for the structuring element (later increased to 20 m)
- “geodesic” for the morphological filtering of the geodesic dilation using a threshold of 2 m for the minimum height of an above ground object relating to its neighbourhood, 50 m for an below ground object/outlier and a segmenting threshold of 1 m for segmentation of the normalized DSM

- “steepedge” for the detection of steep edge ground segments using filter radii 4 and 40 and a height threshold of 5 m (same parameters throughout all analysis)

For this investigation for each of the object types (Forest, Houses, Industry, Urban) the efficiency of each algorithm depending on object type and selected different ground amplitudes are analysed.

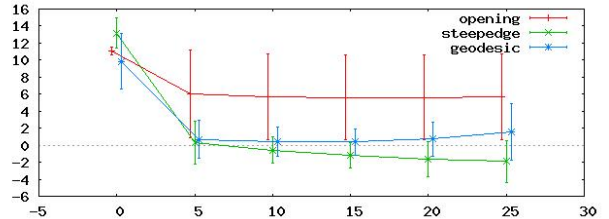


Figure 11: Mean and standard deviation of DTMs extracted from model Forest with method “opening” (red), “steepedge” (green) and “geodesic” (blue) to synthetic DTM plotted against amplitude of synthetic DTM (0: flat to 25: 0 m...50 m)

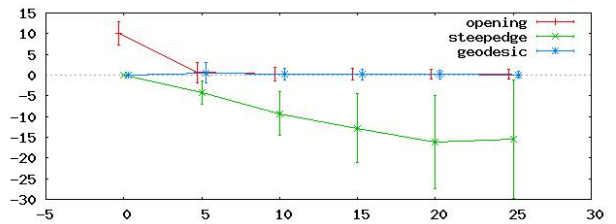


Figure 12: Mean and standard deviation of DTMs extracted from model Houses with method “opening” (red), “steepedge” (green) and “geodesic” (blue) to synthetic DTM plotted against amplitude of synthetic DTM

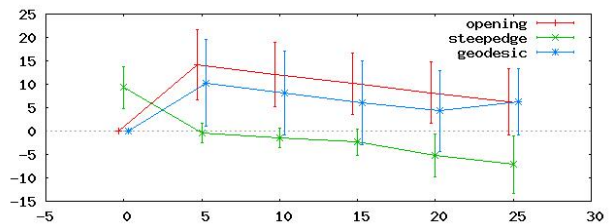


Figure 13: Mean and standard deviation of DTMs extracted from model Industry with method “opening” (red), “steepedge” (green) and “geodesic” (blue) to synthetic DTM plotted against amplitude of synthetic DTM

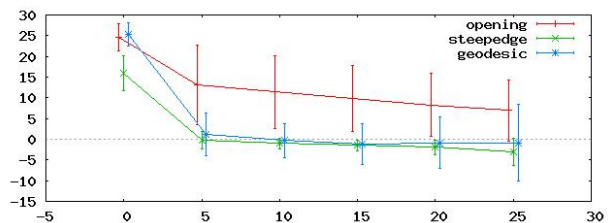


Figure 14: Mean and standard deviation of DTMs extracted from model Urban with method “opening” (red), “steepedge” (green) and “geodesic” (blue) to synthetic DTM plotted against amplitude of synthetic DTM

Figs. 11 through 14 shows the dependency of the means and standard deviations of the generated DTMs with respect to the original synthetic DTM. Here can be seen that the steepedge algorithm fails in the house case since too few “street objects” can be found due to missing steep edges and so the “unknown” (zero) values cause the negative deviations to the original DTM.

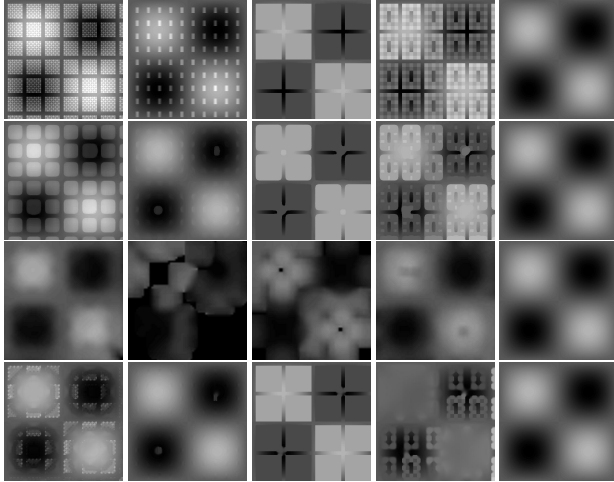


Figure 15: Top row: original synthetic DSMs (left to right: Forest, Houses, Industry, Urban and original DTM); Row 2–4: derived DTMs from the top row using methods “opening”, “steepedge” and “geodesic” respectively; DTM amplitude 25 m

As can be seen in in fig. 15 for scattered small houses both the opening and the geodesic algorithms perform best while the steep edge detection fails completely. On the other hand the steepedge algorithm works best for the modeled kind of forest or typical urban or industrial areas retaining rather good – respectively the best of all poor results.

#### 4.2 Error Dependency

This evaluation analyses the sensitivity of the algorithms to different types of errors and their magnitudes. Following types of errors which occur normally in DSMs generated from stereo satellite imagery using dense stereo algorithms are:

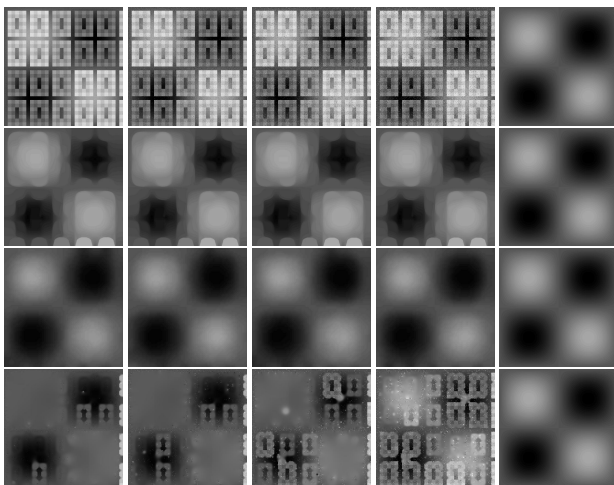


Figure 16: Top: synthetic DSM with noise at level 10, 30, 50, 80 and original DTM; Below: DTM results from opening, steepedge and geodesic calculated for the top DSMs respectively, original DTM; DTM amplitude 20 m

- Noise: positive and negative blunders in DSM at 10 % of

DSM with heights of  $l \cdot r^3$  ( $l$  is level of noise,  $r$  is a random number between 0 and 1)

- Holes: blunders detected and eliminated by dense stereo algorithm (level  $l$  gives the probability of holes in %)
- Occlusions: areas only seen in one of the stereo images and so with unknown height (level  $l$  gives the size of horizontal holes near steep edges in the DSM, depending also on the height change)

In this investigation for better comparison the radius of the structuring element in the opening algorithm is increased to 20 m and the DTM amplitude reduced to also 20 m (heights ranging from 0 to 40 m).

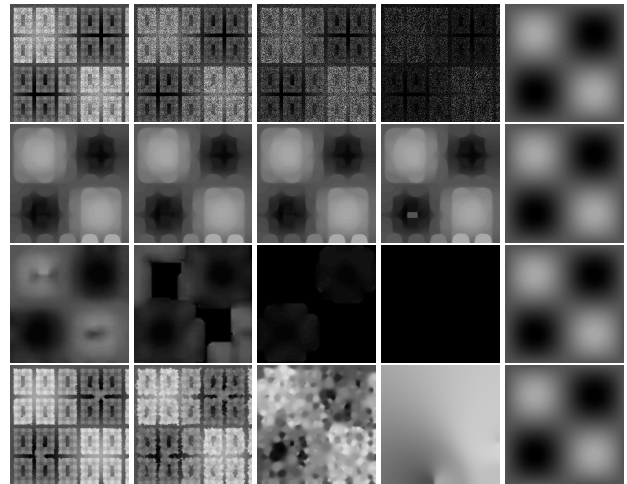


Figure 17: Top: Holes at level 10, 30, 50, 80; Below: DTM results from opening, steepedge and geodesic

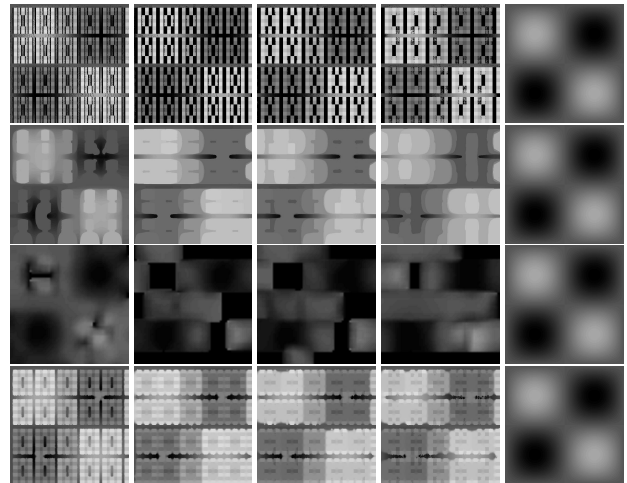


Figure 18: Top: Occlusions at level 10, 30, 50, 80; Below: DTM results from opening, steepedge and geodesic

Figs. 16 to 18 shows the results gained with the different algorithms from the error induced synthetic DSMs. The first row contains in all three cases the generated artificial DSM showing the errors together with the original DTM used on the right hand side. The three rows below show in all three cases the results of the algorithms “opening”, “steep edge” and “geodesic” also together with the original DTM which should result on the right hand side. The following plots in fig. 19 to 21 shows the dependency of the mean and standard deviation values with respect to the original synthetic DTM as a function of the error level  $l$ . In

all plots the “opening” is shown in red, the “steep edge” in green and the “geodesic” in blue.

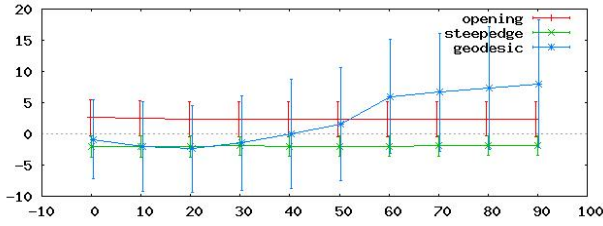


Figure 19: Dependency of mean and standard deviation with respect to synthetic DTM from noise level

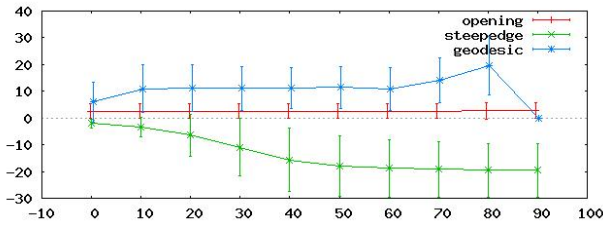


Figure 20: Dependency of mean and standard deviation with respect to synthetic DTM from holes level

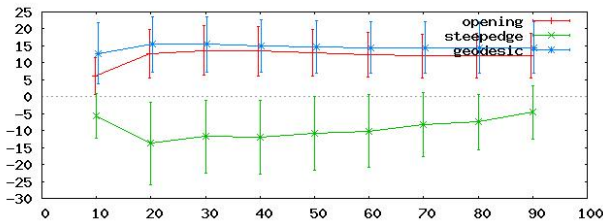


Figure 21: Dependency of mean and standard deviation with respect to synthetic DTM from occlusion level

Positive values in these plots shows objects not removed in the resulting DTM while negative values, which occur mostly with the “steep edge” method, originate from uninterpolated areas which remain the background value 0.

### 4.3 Dependency on DTM undulation frequency

In the last investigation the sensitivity of the algorithms to the changing undulation frequency of the ground is analysed. This is done from none (flat ground) to 7.5 periods in 512 m. In this case for better comparison also a radius of the structuring element in the opening algorithm of 20 m but only a DTM amplitude of 10 m is used. All previous investigations were done with one period in 512 m corresponding to one hill and one dip in each direction. A period of 0.5 corresponds to only one hill of height “amplitude” in the center of the DTM as shown in fig. 23 in the left column.

Fig. 22 shows again the mean and standard deviations of the generated DTMs but this time as a function of the undulation periods of the underlying DTM. In fig. 23 the first row shows the synthetic urban DEM on top of the DTMs with various periods. The three following rows show the extracted DTM results using “opening”, “steep edge” and “geodesic” for the corresponding artificial DSMs.

In periods dependency – caused mainly on the urban type of DEM which provides good steep edges – the “steep edge” algorithm

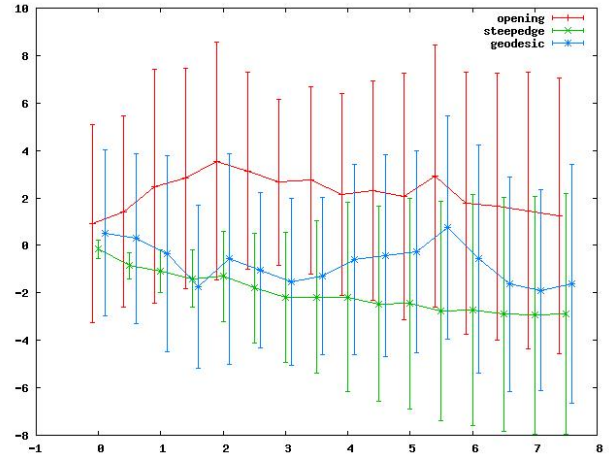


Figure 22: Dependency of mean and standard deviation of calculated DTMs with algorithms opening (red), steepedge (green) and geodesic (blue) from number of periods of DTM

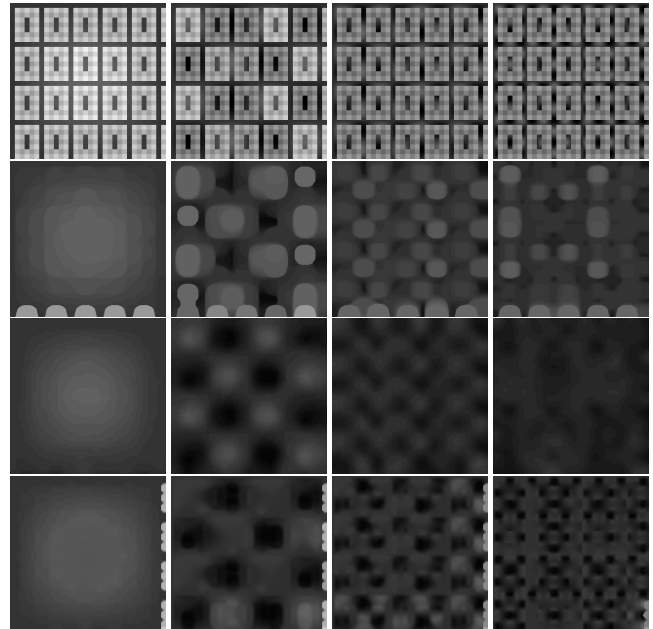


Figure 23: Top: DSMs with periods 0.5, 2, 4 and 7; Below: DTM results from opening, steepedge and geodesic

performs best. Second “geodesic” followed by “opening”. For the last one mentioned this analysis shows clearly the dependency of the good DTM extraction with increasing radius of the structuring element versus the failure of the ability following smaller scale DTM variations.

## 5 DISCUSSION

The simulated cases show some specific situations for urban areas since seldom there will be such steep and on small scale varying DTMs in cities. But nevertheless all three analyzed algorithms show very promising results. The simplest algorithm “opening” works very well for buildings or urban objects with footprints smaller than the diameter of the structuring element.

The second algorithm “steep edge” works very well in cases where steep edges can be found like in urban or industrial areas. The third algorithm “geodesic” is a good trade-off for a general purpose DTM algorithm but also with problems in industrial areas.

The best stability to noise shows the “steep edge” algorithm followed by “opening” which shows also good stability in case of many holes. In the last case the other two algorithms show increasing weaknesses.

For small scale ground undulations the “opening” approach gets more and more weak in contrast to “steep edge” and “geodesic” due to the conflict of a preferably large radius of the structuring element to cover also large buildings but wiping out small scale DTM undulations using such large radii.

## 6 CONCLUSION AND OUTLOOK

In conclusion we can state that all three algorithms work rather good depending on the case. For more open landscape with scattered elevated objects and large scale DTM variations the classical “opening” is absolutely sufficient. In urban cases with steep edges the “steep edge” algorithm shows its strength. The “geodesic” algorithm shows some behaviour in between which improves it as a general purpose solution.

After all we propose the combination of different algorithms which may be specialized for different urban situations. An adaptive solution could be envisaged for future work. On the other hand a direct solution may be: Since the result should be a ground model and if we ensure all algorithms handle negative blunders properly we can assume that the result of an algorithm is better the lower it is. With this assumption the resulting DTM will be a smoothed minimum of all DTMs produced by all used, different algorithms. But care has to be taken on the sensitivity of the methods to outliers below the ground which can result in significant errors or missing values in elevated areas which results in interpolated areas lower than existing hills.

Also – as can be seen in the application of the “steep edge” algorithm to the housing area – a kind of “confidence measure” has to be introduced which shows the reliability of the algorithm in this area. If – for the steep edge example – no steep edges can be found in some area the confidence will disappear and another algorithm should be preferred in such areas. Introducing such confidence measures for different algorithms may lead to a “best of” DTM depending on locally features of the DSM.

## References

- Arefi, H. and Hahn, M., 2005. A morphological reconstruction algorithm for separating off-terrain points from terrain points in laser scanning data. ISPRS.
- Arefi, H., dAngelo, P., Mayer, H. and Reinartz, P., 2009. Automatic generation of digital terrain models from cartosat-1 stereo images.
- Arefi, H., Engels, J., Hahn, M. and Mayer, H., 2007. Automatic DTM generation from laser-scanning data in residential hilly area.
- Axelsson, P., 1999. Processing of laser scanner data algorithms and applications. ISPRS Journal of Photogrammetry and Remote Sensing 54, pp. 138–147.
- Baillard, C., 2008. A hybrid method for deriving DTMs from urban DEMs. Vol. 37, pp. 109–114.
- dAngelo, P., Lehner, M., Krauß, T., Hoja, D. and Reinartz, P., 2008. Towards automated dem generation from high resolution stereo satellite images. Vol. 37, pp. 1137–1142.
- Haralick, R., Sternberg, S. and Zhuang, X., 1987. Image analysis using mathematical morphology. IEEE Trans. Pattern Anal. Machine Intell. 9(4), pp. 532–550.
- Krauß, T. and Reinartz, P., 2009. Refinement of urban digital elevation models from very high resolution stereo satellite images. Vol. 38.
- Krauß, T. and Reinartz, P., 2010. Urban object detection using a fusion approach of dense urban digital surface models and VHR optical satellite stereo data. In: ISPRS Istanbul Workshop 2010, WG I/4 Modeling of optical airborne and space borne sensors, Vol. 39.
- Krauß, T., Lehner, M. and Reinartz, P., 2008. Generation of coarse 3d models of urban areas from high resolution stereo satellite images. Vol. 37.
- Li, Z., Zhu, Q. and Gold, C., 2005. Digital Terrain Modeling - Principles and Methodology.
- Vincent, L., 1993. Morphological grayscale reconstruction in image analysis: applications and efficient algorithms. IEEE Trans Image Process. 1993(2(2)), pp. 176–201.
- Vosselman, G., 2000. Slope based filtering of laser altimetry data. IAPRS XXXIII, pp. 935–942.
- Weidner, U. and Förstner, W., 1995. Towards automatic building extraction from high resolution digital elevation models. ISPRS 50 (4), pp. 38–49.
- Zhang, K., Chen, S., Whitman, D., Shyu, M., Yan, J. and Zhang, C., 2003. A progressive morphological filter for removing non-ground measurements from airborne lidar data. IEEE Trans. on Geoscience and Remote Sensing 41(4), pp. 872–882.